Linearized augmented-plane-wave study of chemisorption of sulfur on Fe(001)

Gayanath W. Fernando* and John W. Wilkins
Laboratory of Atomic and Solid State Physics and Materials Science Center, Cornell University, Ithaca, New York 14853-2501
(Received 15 July 1985)

Self-consistent linearized augmented-plane-wave calculations on $c(2\times2)$S/Fe(001) suggest that the interaction of sulfur with iron is not just limited to the surface atoms but extends to the subsurface layer. A charge buildup occurs between the sulfur and the surface iron atoms, forming a directional bond. A comparison between the calculated sulfur-derived bands and the recent angle-resolved ultraviolet-photoemission-spectroscopy results yields reasonable agreement with the experimental dispersions and the bandwidths; in particular the p_x-p_y bandwidth along $\bar{\Sigma}$ agrees to within 0.2 eV.

I. INTRODUCTION

There has been a great deal of interest recently in surface studies on transition-metal surfaces, especially after the experimentalists began using ultrahigh-vacuum systems, synchrotron radiation, etc. to obtain reproducible results. Although a great deal of experimental and theoretical work has been done on surfaces such as nickel and tungsten, iron still remains less well studied. Iron is a difficult surface to clean, and this is one major reason for the current situation. However, using the new experimental techniques, experimentalists have begun looking into one of the most commonly used surfaces in industry.

Iron plays an important role in ammonia synthesis, in the Fischer-Tropsch process, and in magnetism. In ammonia synthesis (the Haber-Bosch process) NH_3 is produced from its elements using an iron catalyst. Small amounts of sulfur (fractions of a monolayer) are known to poison this iron catalyst.[1] Fischer-Tropsch process is the production of hydrocarbons, alcohols, etc. by CO and H_2 over an iron catalyst. Here too sulfur acts as a poison. The high electronegativity of sulfur is believed to be one reason for its poisoning effect. In alloy steels, diffusion of sulfur to grain boundaries is one of the main causes of temper embrittlement. As a first step toward understanding all of these phenomena, electronic-structure calculations may be used to gather information about charge transfer, surface states, bonding, etc.

A. Method

The calculational method employed here is the linearized augmented-plane-wave (LAPW) method.[2] The basis functions (i) in the interstitial region are plane waves, (ii) inside the muffin-tin sphere, and (iii) in the vacuum region are solutions of the muffin-tin Schrödinger equation (spherically averaged potential inside the spheres and planarly averaged potential in the vacuum). The single-particle Schrödinger equation is solved self-consistently by iterating on the charge density. The effective one-particle potential used in the Schrödinger equation is the sum of the Coulomb potential and the exchange-correlation potential. From the various exchange-correlation potentials that exist in the literature, all based on the free-electron gas, we use Ceperley-Alder-Vosko-Wilk-Nusair exchange-correlation potential.[3]

The calculations described here have the full potential in the interstitial region. However, a plane-wave extension as described by Jepsen, Madsen, and Andersen[2] is used to approximate the non-muffin-tin corrections to the muffin-tin potential, in the sphere and vacuum regions. The angular-momentum cutoff is $l=3$ (i.e., we include up to f waves). The largest reciprocal-lattice vector, $\mathbf{G}_{\max}$, used in our LAPW basis set is chosen such that $R_{\mathrm{MT}}G_{\max}\simeq7.0$, where R_{MT} is the muffin-tin radius of the Fe atom. The final self-consistent results reported are from a 21-**k**-point mesh in the irreducible Brillouin zone. The typical variations between the input and output charge densities at self-consistency are less than $1\times10^{-3}e/a_0^3$.

B. System

Legg, Jona, Jepsen, and Marcus,[4] by comparing low-energy electron-diffraction (LEED) intensity versus energy profiles with theoretical profiles calculated for an assumed structural model, reported seeing a $c(2\times2)$S overlayer on Fe(001) with sulfur occupying the four-fold hollow site at a distance 1.09 Å above the surface plane.

We are presenting results of our calculation for a five-layer film of bcc Fe(001) with sulfur adsorbed on both sides. Figures 1 and 2 show various cuts of the $c(2\times2)$S/Fe(001) system studied. The basis in the unit cell consists of ten iron and two sulfur atoms, but, with the aid of z-reflection (normal to the slab) symmetry it can be reduced to six irons and one sulfur. The two iron atoms on the center plane are equivalent, as are those on the surface plane. However, on the subsurface layer there are two inequivalent iron atoms, one with a sulfur atom directly above and the other with no sulfur directly above (Fig. 2).

II. RESULTS AND DISCUSSION

A. Placement and dispersion of sulfur-derived bands

A comparison of the available experimental dispersions[6] and our calculated sulfur-derived dispersions is shown in

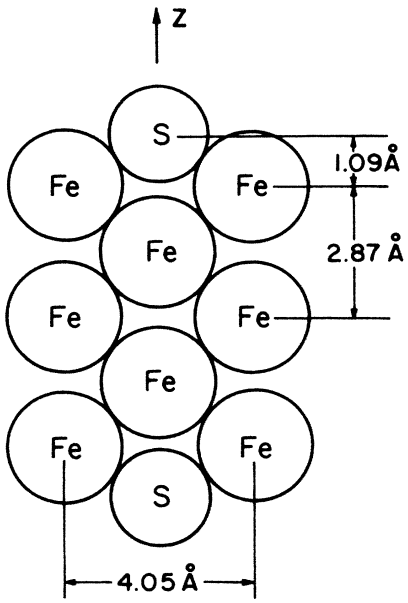

FIG. 1. (110) cut of $c(2\times2)$S/Fe(001) system. z-reflection symmetry is maintained by having two sulfur overlayers on opposing sides of the five-layer iron slab.

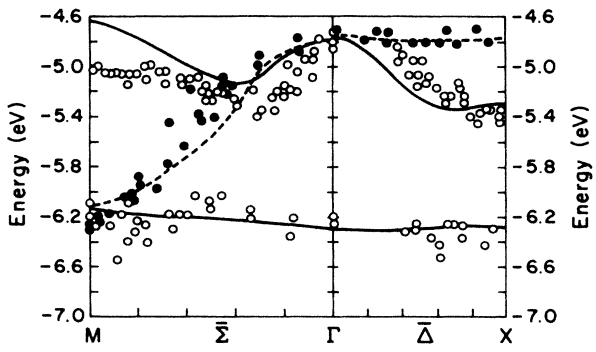

FIG. 3. Comparison of sulfur-derived bands with ARUPS results of (Ref. 6). Solid lines are calculated even bands, while dashed lines are calculated odd bands; ○ and ● denote experimental data corresponding, respectively, to even and odd reflections symmetry about the mirror plane defined by $\bar{\Gamma}\bar{X}$ or $\bar{\Gamma}\bar{M}$, where appropriate. Note that these calculated sulfur-derived bands have been shifted down by 0.8 eV. Energies are measured with respect to the Fermi level. For comparison, our LAPW sulfur *monolayer* calculation, for the same S-S distance, gives bandwidths of 0.7, 0.6, and 1.3 eV at $\bar{M}$, $\bar{\Gamma}$, and $\bar{X}$, respectively. Thus the interaction with the iron appreciably broadens the bandwidth at $\bar{M}$ and $\bar{\Gamma}$, but not at $\bar{X}$.

Fig. 3. In the angle-resolved ultraviolet-photoemission-spectroscopy (ARUPS) experiment, for sets of data at a constant photon energy, the Fermi level was chosen to be at the middle of the Fermi edge from 10% to 90% of its height. This width was typically 0.4 eV, so that the binding energies carry an error of ±0.2 eV. At point $\bar{\Gamma}$, degenerate levels 4.8 eV below the Fermi level are mostly sulfur p_x and p_y, while the level 6.2 eV below the Fermi level at point $\bar{\Gamma}$ is mostly sulfur p_z (z being normal to the slab). At point $\bar{\Gamma}$, the p_x (p_y) level lies above p_z level due to the antibonding overlap of the neighboring sulfur p_x (p_y) orbitals. However, at point $\bar{M}$ this ordering of levels is reversed due to the bonding overlap of the neighboring sulfur p_x (p_y) orbitals.

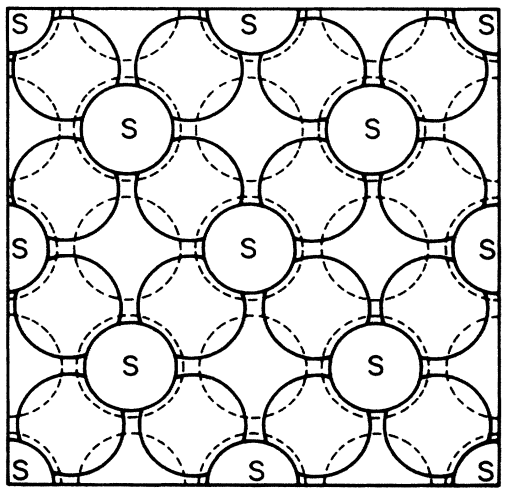

FIG. 2. Top view of $c(2\times2)$S/Fe(001). Solid circles denote the surface Fe and sulfur atoms, while dashed circles denote subsurface-layer Fe atoms. Note that the subsurface layer has two inequivalent Fe atoms, one directly below the sulfur and the other with no sulfur directly above.

The apparent agreement between theory and experiment is achieved by lowering the computed sulfur-derived bands 0.8 eV with respect to the Fermi level. There are several separate and supporting explanations for this seemingly arbitrary shift.

In photoemission, relaxation effects, associated with the screening of a hole created by the photon, lower the binding energies compared to the ones calculated using the effective single-particle potential. As a result, the measured binding energy cannot be directly linked to the calculated (band) energy levels.[7,8]

If only these relaxation effects were taken into account, the measured sulfur p levels ought to lie higher in energy than our calculated ones (i.e., contrary to what is observed). However, there is another effect which produces a shift in the opposite direction in the calculated bands. In the local-density approximation (LDA) the electron is allowed to interact with itself (self-interaction), and the self-interaction correction usually pushes the calculated LDA energy eigenvalues to more negative energies.

Since these two effects are in opposite directions, *sometimes* they cancel each other and apparent agreement is obtained with the single-particle (band-structure) levels. In fact, such comparisons between photoemission results

and band calculations for Cu (as well as many other metals) have been made, and the possible importance of these many-body effects has been raised.[9–12]

It is believed that the shifts associated with the valence d levels are smaller than those seen here for the sulfur p levels. Norman,[12] in his application of a screened self-interaction correction to Cu and Zn, points out that for Cu the $3d$ holes show a comparable relaxation and hence a comparable localization with respect to the screening charge as the $3s$ and $3p$ core hole levels, but argues that the d hole is not so localized in the $3d$ transition metals like vanadium, whose d bands are only partially filled, and have larger dispersions. The local-density error increases as the d bands drop in energy; for example, in Cu the LDA d-band–position error is 0.5 eV, while in Zn it is over 2 eV.[12] On the other hand, comparison of some LDA d-band energy eigenvalues of vanadium with experiment shows excellent agreement.[13] Thus the subject is far from closed.

We think the discrepancy seen in the placement of the sulfur p levels with respect to the Fermi level might be explained in terms of the above-mentioned effects. Note that once the calculated sulfur-derived bands have been shifted down by 0.8 eV, the agreement between the calculated band dispersions and the ARUPS-derived bands is reasonably good. Also, regardless of the above shift the calculated odd p_x-p_y band along $\bar{\Sigma}$, which is degenerate in $+$ and $-$ z-reflection symmetries [see Fig. 9(b)], has a width that agrees to within 0.2 eV with experiment (see Fig. 3).

B. Substrate thickness

We first attempted a calculation of chemisorption of sulfur on an iron substrate that was three layers thick. The five-layer substrate was used after we realized that the sulfur atoms on the opposite sides of the slab were "seeing each other." In the three-layer case sulfur dispersions were seen to be strongly affected by the leakage of "p_z" through the slab. This was most evident in the negative-z-reflection-symmetry, p_z-dominated regions of the bands for the three-layer case. For example, the (p_x,p_y)-p_z separation at Γ was 0.8 eV for the three-layer case, while it was 1.4 eV for the five-layer case. Only p_z-dominated regions were seen to undergo shifts of this magnitude with respect to the corresponding widths for the five-layer calculation. The separations of the two sulfur atoms on the opposite sides was 5.05 Å (three layers of Fe) and 7.90 Å (five layers of Fe), while the nearest-neighbor S-S distance for the overlayer was 4.05 Å.

C. Work function

Adsorption of sulfur on Fe(001) leads to an increase in the work function both experimentally and theoretically. Table I is a summary of experimental and theoretical values for the work function.

The calculated work function of clean iron and sulfur-covered iron shows oscillations with respect to slab thickness. In Refs. 18 and 19 the same group reports a LAPW-calculated work-function *decrease* of 0.3 eV in going from five to seven layers of iron, both ferromagnetic. We noticed a 0.3-eV *increase* in the work function in going from sulfur on three layers of iron to sulfur on five layers of iron.

Recently, Feibelman and Hamann[23] focused their attention on what they called "quantum-size effects" in work functions. In their LAPW study the work function of Cr(001) turned out to be quite stable with respect to slab thickness and resulted in an excellent value compared to experiment, while for Rh(111) it was not stable for two,

TABLE I. Experimental and theoretical work functions for clean iron (001), $c(2\times2)$S/Fe(001), and the work-function change due to a $c(2\times2)$S overlayer on Ni(001).

	Experiment (eV)	Theory (eV)
Fe(001)	4.31[a]	4.2 (5 layers, paramagnetic)[f]
	4.88[b]	4.86 (7 layers, paramagnetic)[g]
	4.67→4.75[c]	4.29 (7 layers, ferromagnetic)[g]
	4.4[d]	4.57 (5 layers, ferromagnetic)[h]
$c(2\times2)$S/Fe(001)	4.66→5.26[c,e]	5.2 (3 layers of Fe)[f]
	(Θ=0→0.65)	5.5 (5 layers of Fe)[f]
Change due to sulfur adsorption on Fe(001)	0.5	1.3
Change due to sulfur adsorption on Ni(001)	0.63[i], 0.38[j]	0.5[k]

[a]Reference 14.
[b]Reference 15.
[c]Reference 5.
[d]Reference 16.
[e]Reference 17.
[f]This work.
[g]Reference 18.
[h]Reference 19.
[i]Reference 20.
[j]Reference 21.
[k]Reference 22.

three, or four layers. There were oscillations of about 0.2—0.3 eV. Finally, when stabilized, it gave a work function of 0.5 eV higher than the experiment. It is argued that for Cr the existence of a surface state right at the Fermi level stabilizes the surface charge density and hence the work function. The surface state at the Fermi level is insensitive to the film thickness. As Cr(001) film thickness increases, the requirement of orthogonality to this surface state forces the new "bulk-state" wave functions to lie in the interior of the film. Thus the surface state stabilizes the dipole layer against quantum-size effects. For the case of Rh, a $4d$-band metal with a high density of states (DOS) at the Fermi level, one may expect small quantum-size effects in the work function, but to the contrary, there are (0.2—0.3)-eV oscillations before the Rh(111) work function stabilizes around seven layers.

We have seen that oscillations in the work function of Fe(001) occur between five- and seven-layer thicknesses. These oscillations may be due to new states that drop through the Fermi level when the film thickness is increased, disturbing the surface dipole layer. Also from Table I, one can see that in going from five to seven layers of Fe(001) there is an increase in the work function in the paramagnetic calculations, while there is a decrease in the work function in the ferromagnetic ones. The new states that drop through the Fermi level are different for the paramagnetic and ferromagnetic slabs, and hence they show different shifts in the work function. From this information we can only give an estimate for the theoretical work function of Fe(001), that lies within the oscillating values, at 4.5 ± 0.3 eV.

A similar effect might occur for sulfur adsorbed on iron. This system also shows an increase of about 0.3 eV in the work function when the iron layer thickness is increased from three to five. Unfortunately, we do not have a computation for seven iron layers. By the way, we doubt that the sulfur p_z levels that leaked through the thinner slab will have any effect on the work function as they do not lie close to the Fermi level. In any case, a reasonable estimate for the calculated work function of $c(2\times2)$S/Fe(001) would be 5.2 ± 0.3 eV.

Work-function measurements for sulfur on Fe(001) have been carried out by Ueda and Shimizu[5] and their measured values are sensitive to sample preparation. Fowler's isotherm method[7] was used in measuring the work function, and the sulfur overlayer was formed by surface segregation. The experimental work-function change given in Table I, i.e., from 4.66 eV at $\Theta_S=0$ (where Θ_S is sulfur coverage) to 5.26 eV at $\Theta_S=0.65$, was seen to depend linearly on coverage, except around zero coverage where some carbon impurities distorted the linearity.

D. Chemisorption of nonmetal atoms and ferromagnetism

Chemisorption of H_2 and CO on thin nickel and iron films has been seen to reduce ferromagnetism in FMR (ferromagnetic resonance) experiments.[24] When d bands near the Fermi level are pulled down to form bonds with an adsorbate, one may expect a reduction in the surface magnetic moment. The above-mentioned chemisorption processes are reversible, but if these Ni and Fe films are exposed to oxygen, irreversible formation of oxide layers takes place. Here too there is a reduction in the surface magnetic moment. Various theoretical attempts exist in the literature to describe chemisorption on transition-metal surfaces. Varma and Wilson[25] were able to produce some systematics of the binding energies of oxygen and hydrogen on $3d$ and $4d$ transition metals. Using a few parameters, such as the bandwidth, mean energy, and Fermi energy, and treating the metals paramagnetically, they were able to achieve reasonable agreement with experimental binding energies. Moran-Lopez and Falicov,[26] through a self-consistent model of hydrogen chemisorption on transition-metal surfaces, based on an Anderson-Hubbard Hamiltonian, and the cluster—Bethe-lattice approximation, found that, in the case of a ferromagnetic substrate for a certain range of values of t_a, the hopping integral for the electronic transition between an atom and substrate, the value of the magnetic moment of the metal atom below the adsorbate increases upon chemisorption.

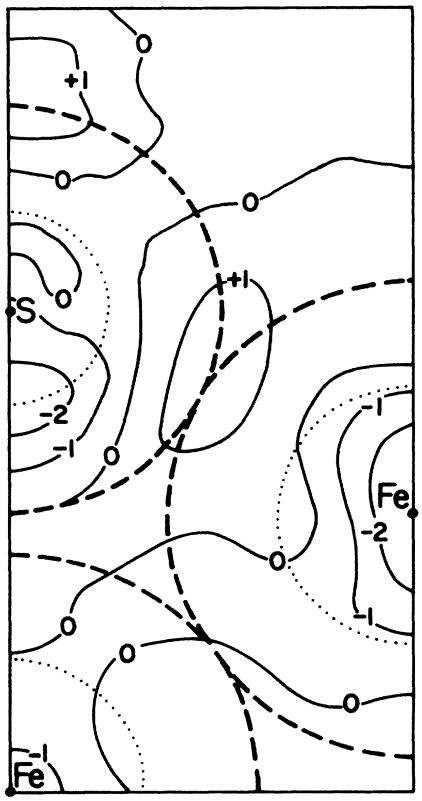

FIG. 4. Changes in electron density of an iron slab upon sulfur adsorption. Electron-density difference between a self-consistent $c(2\times2)$S/Fe(001) calculation and a self-consistent five-layer Fe(001) calculation and an isolated sulfur atom has been plotted in units of $0.01e/a_0^3$. This is a (110) cut and shows a surface Fe atom as well as a subsurface-layer Fe atom directly below sulfur. The dashed lines indicate the MT sphere boundaries, while the dotted lines show where the frozen-core density has dropped to $0.1e/a_0^3$. Note the charge buildup between sulfur and the surface Fe atom giving rise to a directional bond.

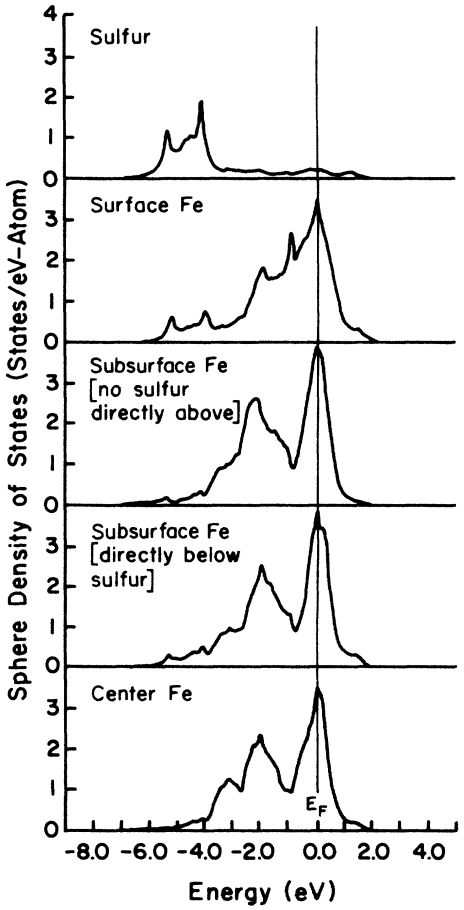

FIG. 5. $c(2\times2)$S/Fe(001) sphere-projected density of states. These have been smoothed by a Lorentzian broadening function of full width at half maximum 0.2 eV.

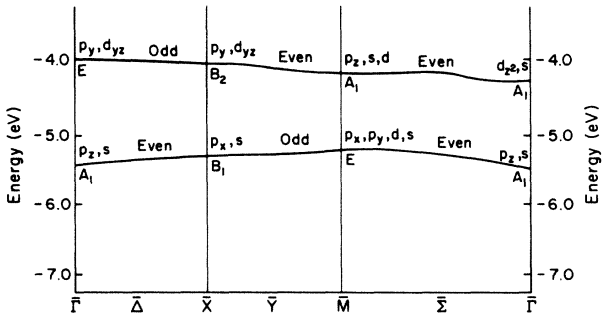

FIG. 6. Energy dispersions (relative to the Fermi level) of the two almost flat bands giving rise to peaks in the sulfur density of states. Odd and even refer to reflection symmetries about the mirror planes defined by $\bar{\Gamma}\bar{X}$ or $\bar{X}\bar{M}$ or $\bar{\Gamma}\bar{M}$, where appropriate. Symmetry labels and dominant orbital characters (sulfur $3p$ and iron $3d$ or $4s$) at the high-symmetry points $\bar{\Gamma}$, $\bar{X}$, and $\bar{M}$ are also shown. This figure contains a different (even) upper band along $\bar{M}\bar{\Gamma}$, from the bands shown in Fig. 3. In fact, there is more than one p_z-derived (or p_x-derived, etc.) occupied band in the band structure. The reason for having more than one p_z-derived band here is due to having overlayers of sulfur on both sides of the five-layer slab. In our thin film there is some leakage of the p_z orbital through the slab, giving rise to a direct p_z overlap (which is very weak here). In addition, there is an indirect effect on the p_z levels due to z reflection restrictions on the other substrate orbitals with which the p_z orbital can mix. Either of these effects will give rise to a splitting between the $+z$- and $-z$-reflection—symmetry bands. For an infinitely thick iron film these splittings would vanish.

There is another range in which the effect is opposite. However, for values of t_a corresponding to Fe, Co, and Ni the magnetic moment of the metal atom below the adsorbate showed a small decrease.

Recently, Wienert and Davenport[27] performed a self-consistent spin-polarized LAPW calculation for H/Ni(001) and found a substantial reduction in the surface Ni magnetic moment. (It was as small as 0.2 bohr magnetons; bulk Ni magnetic moment is 0.6 magnetons.) This calculation is far more accurate than any of the other calculations described above and confirms the FMR experimental results of Ref. 24. These results provide a justification for doing paramagnetic calculations for the chemisorption of nonmetal atoms on transition-metal surfaces. To quote Varma and Wilson[25] on this: "We should have, in principle, distinguished the interaction between orbitals with the same z component of spins and those with different z component of spins by introducing an exchange energy. If the adsorption (chemisorption of hydrogen and oxygen on transition metals) is, as we believe, to a state of zero total spin, this would have merely introduced an additional parameter without adding any essential new insight." Our calculation also supports this view. The sulfur-derived band separation and dispersions agreed

TABLE II. Symmetry analysis of the two almost flat bands giving rise to peaks in sulfur density of states. Orbitals that contribute at least 15% from the total sphere charge are listed and orbital character is given in parenthesis. Fe below S refers to the iron atom directly below sulfur in the subsurface layer.

Approximate band position (eV)	$\bar{\Gamma}$ Neighborhood Surface	$\bar{X}$ Neighborhood Surface	$\bar{M}$ Neighborhood Center	$\bar{M}$ Neighborhood Below S
−4.0	S($3p_y$), Fe($3d$)	S($3p_y$), Fe($3d$)	Fe($3d$),	Fe($4s$), S($3p_z$)
	Below S Surface	Surface	Surface	
−5.4	S($3p_z$), Fe($4s$), Fe($4s$)	S($3p_x$), Fe($4s$)	Fe($3d,4s$),	S($3p_x,3p_y$)

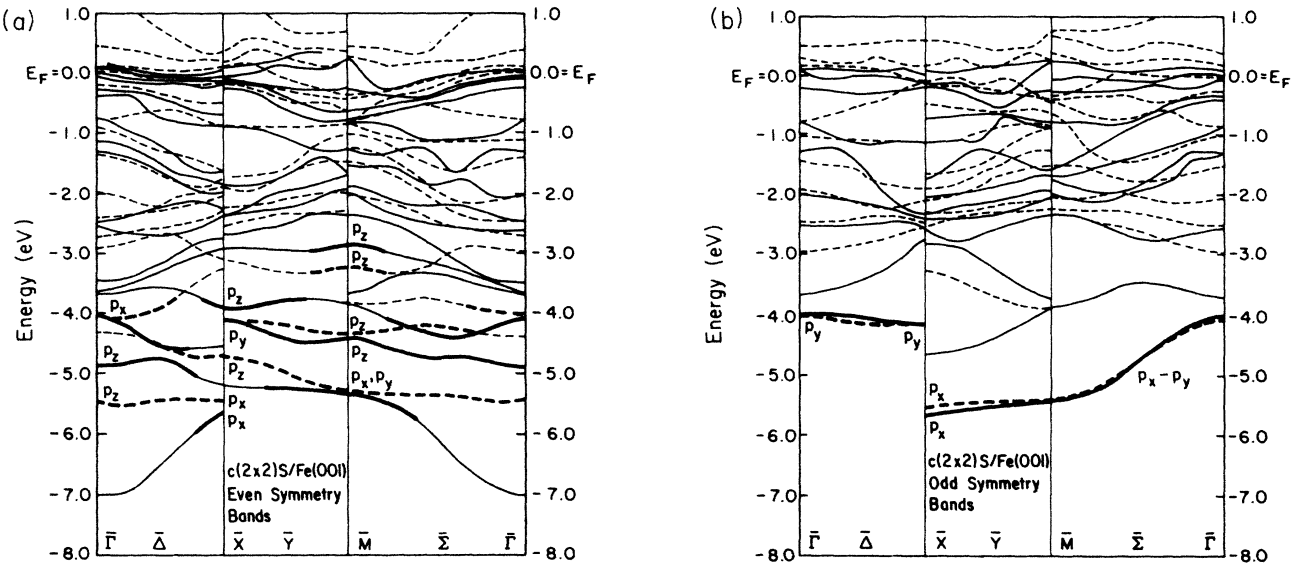

FIG. 7. Calculated $c(2\times2)$S/Fe(001) (a) even and (b) odd symmetry bands. Sulfur-derived levels with more than 20% weight in the sulfur muffin-tin sphere (compared to the total muffin-tin sphere weight) have been darkened and corresponding sulfur $3p$ character indicated. Solid and dashed lines refer to + and − z-reflection symmetries.

reasonably well with experiments. Also, the work-function values for the chemisorbed and clean cases were certainly not wildly different from the experimental values.

E. Changes due to chemisorption

Large LAPW calculations generate a large number of potentially interesting quantities. It is important to look at their collective implications before coming to conclusions. The large change in work function is due to a large dipole layer at the surface. The difference density contours (Fig. 4) indicate that sulfur atoms as well as nearby iron atoms lose valence density from their interior to bonding regions and to a region directly above the sulfur atom. The work-function change is likely to be associated with these redistributions of charge near the surface region.

A reasonable view of the chemisorption bond could be obtained by looking at the difference density contours

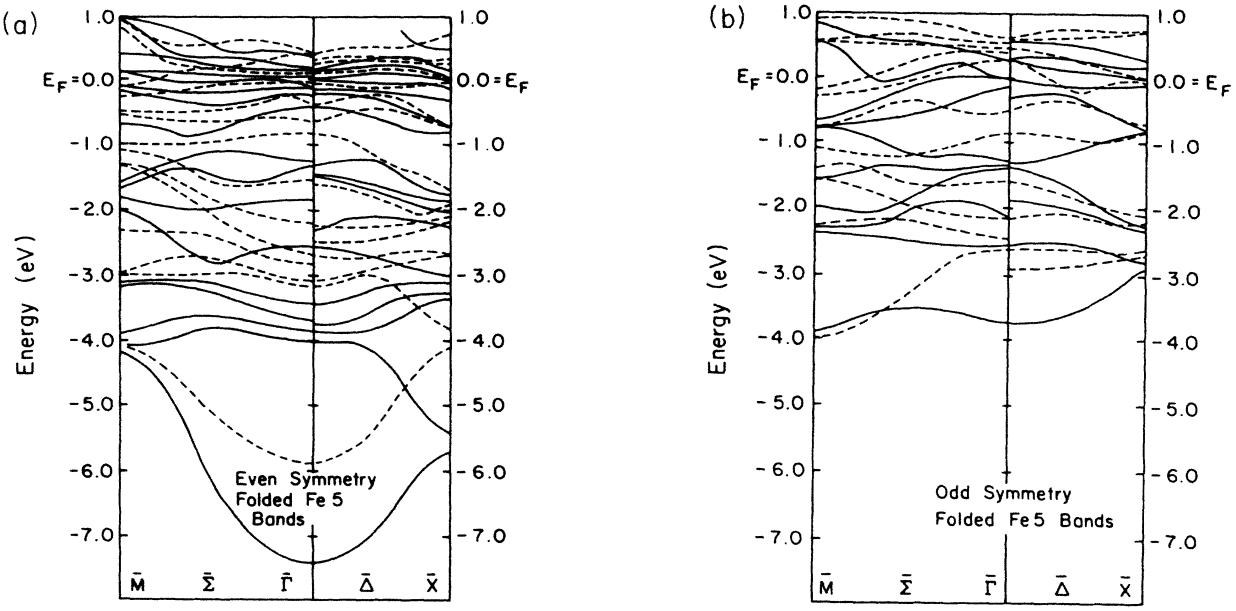

FIG. 8. Calculated Fe(001) five-layer (a) even and (b) odd symmetry bands folded into the $c(2\times2)$ overlayer zone. Solid and dashed lines refer to + and − z-reflection symmetries, respectively.

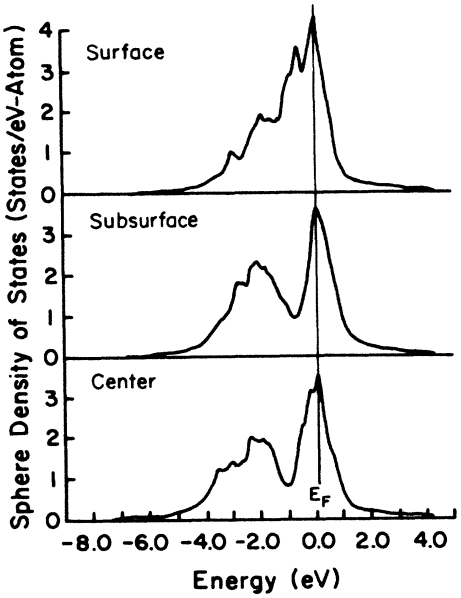

FIG. 9. Sphere-projected density of states for five-layer iron slab. These have been smoothed by a Lorentzian broadening function of full width at half maximum 0.2 eV.

(Fig. 4), sphere-projected DOS curves (Fig. 5), sulfur-derived bands (Figs. 3, 6, and 7), and clean iron bands (Fig. 8). The d_{xz} and d_{yz} orbitals of the surface Fe atoms form directional bonds with the sulfur p_x and p_y orbitals. Along $\bar{\Delta}$ the flat band at 4.0 eV below Fermi energy is almost entirely (p_y,d_{yz}) character from the sulfur and the surface iron atoms, respectively.

Table II gives a detailed description of the relative contribution of the various orbitals to the two flat sulfur-derived bands at 4.0 and 5.4 eV below the Fermi level around points $\bar{\Gamma}$, $\bar{X}$, and $\bar{M}$. In addition to these there are other sulfur-derived bands in the region -4.0 to -5.4 eV. A symmetry analysis and a projection into various (sphere and angular momentum, etc.) sums show that the dominant contributions to those bands come from the surface Fe d orbitals, as well as from the Fe atom directly below sulfur through its $4s$ and d_{z^2} orbitals and sulfur p_z, p_x, and p_y orbitals.

It is also interesting to note that our LAPW calculation for a sulfur *monolayer*, with the overlayer nearest-neighbor distance 4.05 Å used here, gave $3p$-band widths at $\bar{\Gamma}$ and $\bar{M}$ which are smaller by 1 eV or so compared to the chemisorbed sulfur-derived bandwidths. The interaction with the iron substrate increases the sulfur bandwidths substantially.

Table III is a summary of some of the important single-number results. Surface iron charge is seen to increase by 0.2 electrons when sulfur is chemisorbed. A substantial increase in the charge density near the bonding regions of the surface Fe and the sulfur atom helps this change. Also, there is a 0.2 electron increase in the chemisorbed sulfur atom compared to the sulfur monolayer calculation mentioned earlier. These, together with the work-function change, support that claim that there is a charge transfer toward the surface when sulfur is chemisorbed on Fe(001).

F. Density of states and poisoning

Sphere-projected DOS curves for the five layers of iron are compared with those after chemisorption of sulfur (Figs. 5 and 9). The two main peaks in the sulfur DOS at 4.2 and 5.4 eV below the Fermi level correspond to two almost flat bands discussed earlier. We do not see any substantial changes in the DOS's of Fe atoms at the Fermi level when sulfur is adsorbed. This is in contrast to the S/Rh(001) work reported by Feibelman and Hamann.[28] In their LAPW calculation (with the Rh substrate two layers thick) the sphere-projected DOS's of Rh atoms undergo substantial reduction at the Fermi level, and the work-function change due to sulfur adsorption is -0.2 eV. Even though there is essentially no work-function change, it is claimed that sulfur does poison Rh through the changes in DOS near the Fermi level. By lowering the

TABLE III. Some of the important single-number results for the various systems studied. Note that there is a 0.2 electron increase in both surface Fe charge and in sulfur sphere charge due to sulfur chemisorption on iron. A sulfur monolayer calculation was done for the S-S nearest-neighbor distance corresponding to $c(2\times2)$S/Fe(001).

System	Work function (eV)	Average interstitial potential (eV)	Bottom of Fe 4s band (eV)	Center sphere charge (electrons)	Subsurface S atom above (electrons)	Fe charge no S atom above (electrons)	Surface Fe charge (electrons)	Sulfur charge (electrons)
	(with respect to vacuum)							
Fe monolayer	5.0	−9.3	−8.4	6.56			6.56	
Fe 5 layers	4.2[a]	−11.1	−11.6	7.06	7.05	7.05	6.83	
$c(2\times2)$S/Fe(001)								
3 layers of Fe	5.2	−10.1	−11.4	7.11	7.11	7.02	7.04	3.81
5 layers of Fe	5.5	−11.0	−12.5	7.04	7.08	7.03	7.04	3.80
Sulfur monolayer	7.2	−6.3						3.57

[a]Experimental values range from 4.31 to 4.88; see Table I.

DOS near the Fermi level, the ability of Rh atoms to respond to external perturbations has decreased.

In the case of $c(2\times2)$S/Fe(001), we see a 1.3-eV increase in the work function and small changes in sphere-projected DOS at the Fermi level. Once sulfur is adsorbed, it is harder for the electrons to leave the surface, and this has a negative effect in catalysis. For example, this poisoned surface will not help dissociation of gaseous molecules like CO and N_2, since it cannot donate electrons readily to the antibonding orbitals of the molecule—a process that helps dissociation.

When the changes in DOS between clean and chemisorbed cases are considered, one can see that the surface Fe atoms have lost weight just below the Fermi level, and gained weight around 4.0 and 5.4 eV below the Fermi level; the d_{xz} and d_{yz} orbitals of the clean Fe atom have been pulled down to form bonds with sulfur. Also, one notices the changes in DOS of the Fe atom directly below sulfur in the subsurface layer. This Fe atom loses weight around 3 eV below the Fermi level (which roughly corresponds to the d_{z^2} position in the clean atom), and gains weight around 4.0 and 5.4 eV below the Fermi level.

For $c(2\times2)$S/Ni(001), it has been seen from a similar calculation[22] that sulfur forms a directional bond with the surface nickel d orbitals, but it does not have a significant interaction with the subsurface Ni atoms. This is at least partly due to differences in fcc and bcc structures. In the bcc structure the subsurface atoms are more exposed to the vacuum, due to the more open surface, and hence adsorbates can interact with the subsurface easier.

III. CONCLUSIONS

The important conclusions from the above results are as follows:

(i) $3d_{xz}$ and $3d_{yz}$ orbitals of the surface iron atoms hybridize strongly with the sulfur $3p_x$ and $3p_y$ orbitals to form directional bonds.

(ii) A sulfur atom also interacts with the subsurface layer, mainly through the $4s$ and $3d_{z^2}$ orbitals of that layer iron atom directly below sulfur.

(iii) There is evidence for charge transfer toward the surface and for poisoning the clean iron surface due to the chemisorbed sulfur.

(iv) The reasonable agreement of the calculated sulfur p-level dispersions and level separations with experiment supports our belief that paramagnetic chemisorption calculations for ferromagnetic iron can be trusted to predict the correct physics. Other studies show that chemisorption usually leads to a reduction in the surface magnetic moment and, hence, magnetic effects may not be very important in the search for changes due to chemisorption.

ACKNOWLEDGMENTS

We have benefited from discussions with Roy Richter and Cyrus Umrigar. We would like to thank E. W. Plummer and R. A. DiDio for providing copies of their work prior to publication. This work was supported by the National Science Foundation through the Materials Science Center at Cornell University.

*Present address: Department of Physics, West Virginia University, Morgantown, WV 26506.

[1]For a review of sulfur poisoning, see L. L. Hegedus and R. W. McCabe, Catal. Rev. Sci. Eng. **23**, 377 (1981).

[2]O. K. Andersen, Phys. Rev. B **12**, 3060 (1975); O. Jepsen, J. Madsen, and O. K. Andersen, *ibid.* **26**, 2790 (1982).

[3]S. H. Vosko, L. Wilk, and N. Nusair, Can. J. Phys. **58**, 1200 (1980).

[4]K. O. Legg, F. Jona, D. W. Jepsen, and P. M. Marcus, Surf. Sci. **66**, 25 (1977).

[5]K. Ueda and R. Shimizu, Jpn. J. Appl. Phys. **12**, 1869 (1973).

[6]R. A. DiDio, Ph.D. thesis, University of Pennsylvania, 1983; R. A. DiDio, E. W. Plummer, and W. R. Graham, Phys. Rev. Lett. **52**, 683 (1984).

[7]R. H. Fowler, Phys. Rev. **38**, 45 (1931).

[8]E. W. Plummer and W. Eberhardt, in *Advances in Chemical Physics,* edited by I. Prigogine and S. Rice (Wiley, New York, 1982), Vol. 49, p. 537.

[9]R. P. Messmer, T. C. Caves, and C. M. Kao, Chem. Phys. Lett. **90**, 296 (1982).

[10]E. Dietz and D. E. Eastman, Phys. Rev. Lett. **41**, 1674 (1978).

[11]R. Courths, V. Bachelier, B. Cord, and S. Hufner, Solid State Commun. **40**, 1059 (1981).

[12]M. R. Norman, Phys. Rev. B **29**, 2956 (1984).

[13]M. Norman and D. D. Koelling, Phys. Rev. B **28**, 4357 (1983).

[14]V. S. Fomenko, in *Handbook of Thermionic Properties,* edited by E. G. V. Samsanow (Plenum, New York, 1966).

[15]H. Kobayashi and S. Kato, Surf. Sci. **12**, 398 (1968).

[16]A. M. Turner, Yu J. Chang, and J. L. Erskine, Phys. Rev. Lett. **48**, 348 (1982).

[17]K. Ueda and R. Shimizu, Surf. Sci. **43**, 77 (1974).

[18]S. Ohnishi, A. J. Freeman, and M. Weinert, J. Magn. Magn. Mater. **31-34**, 889 (1983); Phys. Rev. B **28**, 6741 (1983).

[19]S. Ohnishi, M. Weinert, and A. J. Freeman, Phys. Rev. B **30**, 36 (1984).

[20]H. D. Hagstrum and G. E. Becker, J. Chem. Phys. **51**, 1015 (1971).

[21]S. E. Demuth and T. N. Rhodin, Surf. Sci. **45**, 269 (1974).

[22]R. Richter and J. W. Wilkins, J. Vac. Sci. Technol. A **1**, 1089 (1983); R. Richter (private communication).

[23]P. J. Feibelman and D. R. Hamann, Phys. Rev. B **29**, 6463 (1984).

[24]W. Göpel, Surf. Sci. **85**, 400 (1979).

[25]C. M. Varma and A. J. Wilson, Phys. Rev. B **22**, 3795 (1980).

[26]J. L. Móran-López and L. M. Falicov, Phys. Rev. B **26**, 2560 (1982).

[27]M. Weinert and J. W. Davenport, Phys. Rev. Lett. **54**, 1547 (1985).

[28]P. J. Feibelman and D. R. Hamann, Phys. Rev. Lett. **52**, 61 (1984).